Research Square

Preprints are preliminary reports that have not undergone peer review.
They should not be considered conclusive, used to inform clinical practice,
or referenced by the media as validated information.

Interfacial Thermal Conductance Due To Electronic Heat Transport Across A Normal-metal to Superconductor Boundary Of Dissimilar Materials

Robert Young

young.rbg@gmail.com

Northrop Grumman Corp.

Research Article

Keywords: Interfacial thermal resistance, thermal boundary resistance, heat transfer coefficient, specific contact resistance, NS contacts, normal-insulator-superconductor junctions, NIS junctions, tunnel junctions, heat flux, heat transport

Posted Date: July 24th, 2026

DOI: https://doi.org/10.21203/rs.3.rs-10061194/v1

License: This work is licensed under a Creative Commons Attribution 4.0 International License.
Read Full License

Additional Declarations: No competing interests reported.

INTERFACIAL THERMAL CONDUCTANCE DUE TO ELECTRONIC HEAT TRANSPORT ACROSS A NORMAL-METAL TO SUPERCONDUCTOR BOUNDARY OF DISSIMILAR MATERIALS

Robert M. Young

Northrop Grumman Corp.

Keywords: Interfacial thermal resistance; thermal boundary resistance; heat transfer coefficient; specific contact resistance; NS contacts; normal-insulator-superconductor junctions; NIS junctions; tunnel junctions; heat flux; heat transport.

Abstract

Over the course of six decades numerous thermal heat transport measurements across a normal-metal to superconductor interface have shown that attributing this transport exclusively to lattice vibrations (phonons), typically taken proportional to the cube of the temperature (T^3), is inadequate. These researchers deemed their results inexplicable, but stating that extra heat transport as carried by electrons would be a likely transport mechanism. Examining the historical thermal data taken on eleven different samples is here compared against four sets of theoretical models that could account for the electronic component: (1) Andreev transport, (2) thin oxide tunneling as proposed by Griffin and Maki, (3) tunneling across an insulating layer as expounded by Giaever and Megerle, and (4) electron scattering at interfacial defects or impurities as considered by Bardeen, Rickayzen, and Teword (BRT). In the cases of the Giaever-Megerle and BRT, determination of the interfacial thermal conductances is newly presented here by means of combination with the Wiedemann-Franz (WF) law as applied to interfaces. Thermal transport is analyzed as the sum of the parallel phonon and electron components across the boundary. Below approximately 20% of T_c interfacial heat transport is dominated by phonons, and it is seen in this work that the contribution due to electrons will often exceed that of the phonon contribution starting at 30% of T_c and dominates above 50%. For $0.2 < T/T_c < 0.5$ both transport mechanisms must be accounted for to align with experiment. This comparison shows that of the four examined interfacial electronic transport models, that of Griffin and Maki does not align well with experiment, that of Andreev can align only if the contacting normal-metal to superconductor area is reduced to a scale 1% or smaller of the physical area and completely fails near and above T_c. Using the interfacial WF law, both adaptations of Giaever-Megerle and BRT enable calculation of the interfacial thermal conductance continuously above and below T_c. Fitting these theoretical models to the experimental thermal data indicates that it is possible that more than one electronic heat transport mechanism may be present simultaneously in some combination. When selecting only one electronic transfer model to combine with the phonon transport, the BRT as adapted using the interfacial WF law requires only a single input, described here as an electrical contact resistance, to adequately cover the full range of temperatures from above T_c in the fully normal state down through T_c and below.

Introduction

The transport of heat across a normal-metal to a dissimilar normal-metal interface is dominated by electrons as the heat carriers, typically far exceeding that of phonons. By contrast, if one of the materials is a dielectric then electron coupling to phonons and phonon transport across the interface will move the heat. In the case of a normal-metal to superconductor boundary the electrons in the superconductor begin to freeze out into Cooper pairs as the temperature is lowered below the superconducting transition temperature T_c. The Cooper pairs do not carry heat, but the unpaired electrons present as quasi-particles still do. Well below T_c the lattice vibrations become dominant, with the boundary transport transitioning towards that of a normal-metal in contact with a dielectric.

The electrical current and voltage across a normal-metal to superconductor interface has been studied[1], but that of the flow of heat imposed by a temperature difference much less so. No present theory describes the thermal boundary resistance (TBR) fully from the normal case down in temperature through T_c and lower. The present work examines experimental data from the literature and attempts to fit existing or modified theory to explain the observed interfacial thermal conductance (ITC).

Theory

In 1964 Andreev[2] originated a theory that explained the extra thermal resistance observed in the experimental data of a tin (Sn) wire that, under the action of an applied magnetic field below the critical field, was in the intermediate state such that a set of regularly spaced sections of normal metal and superconductor occurred along the length of the wire. Andreev's original equation was for a single material, not two dissimilar ones in contact, and for temperatures below $T_c/2$. This was extended by Bonnard, Laeng, Suter, and Rinderer[3] for temperatures closer to T_c. Since most of the experimental data in the literature is plotted as interfacial thermal conductance (ITC, but also commonly called the heat transfer coefficient, or HTC), namely the inverse of the interfacial thermal resistance, this extended equation can be written as:

$$1/R_{th,es}^{A"} = G_{th,es}^{A"} = \frac{f_0 k_F^2 k_B^2}{h\sqrt{\pi}}\left(\frac{\Delta}{k_B} + \frac{3}{2}T\right)\sqrt{\frac{\Delta}{k_B T}}\; exp(^{-\Delta}/_{k_B T})$$

Equation 1

Here $G_{th,es}^{A"}$ [W/cm^2-K] represents the interfacial thermal conductance due to Andreev effects of electrons at the interface between the normal state material and the superconducting state material. In this form the gap is in Joules, temperature in Kelvin, Planck's constant in J-s, the Fermi wavevector in cm^{-2} and Boltzmann's constant in J/K. Bonnard and co-workers found, working with homogeneous samples rendered by a sub-critical magnetic field into alternating layers of superconductor and normal material, that Equation 1 under predicts for $T/T_c < 0.3$, presuming that a phonon heat transport term needs to be added. This will be shown to be also the case when analyzing the dissimilar metal interfacial heat transfer in the next section. For that analysis the experimentally determined values as found by Bonnard and co-workers for lead[3] f_0^{Pb} = 1.13 and f_0^{Sn} = 1.0 for Sn[4] will be used.

Shortly after Andreev's publication, Griffin and Maki[5] examined an interfacial resistance that, starting above T_c in the completely normal region, would cover the transition to below T_c, and for dissimilar metals. Taking that quantum-mechanical tunneling of the electron heat current between a superconductor and a normal metal separated by a very thin oxide layer as a mechanism for the heat transfer, they derived for low temperatures Equation 2. (Note that their analysis did not elucidate higher order terms of the nature of $\{1 + O(k_BT/\Delta)\}^{-1}$so this has been taken as simply 1 for comparisons beyond the low temperature portion.)

$$\left(R_{th,es}^{GM,low}\, A_c^{GM,low}\right)^{-1} = {G_{th,es}^{GM,low}}\Big/_{A_c^{GM,low}} = \frac{4\pi^2 k_B^2}{e^2} T \left(\frac{1}{R_n^{GM,low} A_c^{GM,low}}\right) \left(\frac{\Delta}{k_B T}\right)\left(\frac{\Delta}{\pi k_B T}\right)^{3/2} exp\left({-\Delta}/{k_B T}\right)\{1 + O(k_BT/\Delta)\}^{-1}$$

Equation 2

Griffin and Maki also derived a high temperature limit equation for behavior near T_c, Equation 3. (Again note that they did not elucidate higher order terms in $\{1 - (3/2)(\Delta/\pi k_B T)^2 + O(\Delta/\pi k_B T)^4\}$ so this will be taken as $\{1 - (3/2)(\Delta/\pi k_B T)^2\}$ when plotting for comparisons near T_c.) A key observable prediction of this theory was an anomalous increase in thermal interfacial conductance just below the transition temperature.

$$\left(R_{th,es}^{GM,high}\, A_c^{GM,high}\right)^{-1} = {G_{th,es}^{GM,high}}\Big/_{A_c^{GM,high}} = \frac{\pi^2 k_B^2}{3\, e^2} T \left(\frac{1}{R_n^{GM,high} A_c^{GM,high}}\right) \left\{1 - \frac{3}{2}\left(\frac{\Delta}{\pi k_B T}\right)^2 + O(\Delta/\pi k_B T)^4\right\}^{-1}$$

Equation 3

Bardeen, Rickayzen, and Tewordt's 1959 paper[6] considered the bulk thermal conductivity [W/m-K] and gave what is here Equation 4 (3.6 in the original paper) as the ratio of the thermal conductivity considering quasi-particles as the heat carriers in a superconductor to that of a normal metal's electrons as heat carriers, often referred to as the BRT equation.

$$\frac{K_{th,es}^{BRT}}{K_{th,en}} = \frac{12}{\pi^2}\left\{F_1(-y) + y\, ln(1 + exp(-y)) + \frac{1}{2} y^2/(1 + exp(y))\right\}$$

Equation 4 – The ratios of thermal conductivities in the superconducting and normal states as per Bardeen, Rickayzen, and Tewordt[6] .

Here $y = \Delta/k_BT$ where the superconducting gap Δ is a function of the temperature, and $F_1(-y) = \int_0^\infty \frac{z\, dz}{1+\exp(1+y)}$.

Equation 4 was derived for bulk thermal conductivities. Challis and Cheeke[7] and Schumann et al.[8] both pointed out that if the heat transfer is controlled by electron scattering at defects in the interface, then it is possible that the BRT equation could be used to calculate the heat transfer across a normal to superconducting interface. In the present context this will indeed be adapted to interfacial thermal conductance and used to explain hitherto inexplicable experimental measurements taken from the

literature at such superconductor to normal-metal interfaces. To do this we begin by stating that the Wiedemann-Franz law for normal-metals, which was originally used to describe the relationship between the bulk thermal conductivity and bulk electrical conductivity, has also been shown recently applicable for the interfacial conductance's of dissimilar normal-metals[9,10,11]. Equating the thermal conductivity ratio $K_{th,es}^{BRT}/K_{th,en}$ with the conductance ratio $G_{th,es}^{BRT}/G_{th,en}$ where G is in units of W/K, and then applying the Wiedemann-Franz law to the normal metal, and subsequently equating the normal metal's electrical conductance $G_{e,en}$ with the interfacial contact resistance *Rc* and the electrical contact resistance times area product *RcA* (the specific resistance, which is the inverse of the electrical conductance per unit area) results in Equation 5:

$$\frac{K_{th,es}^{BRT}}{K_{th,en}} = \frac{G_{th,es}^{BRT}}{G_{th,en}} = \frac{G_{th,es}^{BRT}}{L_o G_{e,en} T} = \frac{G_{th,es}^{BRT}}{\left({L_o T}/{R_c^{BRT}}\right)} = \frac{G_{th,es}^{BRT}}{(\mathbb{h}' T)} = \frac{{G_{th,es}^{BRT}}/{A_c^{BRT}}}{\left(\frac{L_o T}{R_c^{BRT} A_c^{BRT}}\right)}.$$

Equation 5

In the above equation $G_{th,en}$ is the interfacial thermal conductance due to electrons as heat carriers in the normal state with the Lorenz constant $L_o = (\pi^2/3)(k_B^2/e^2)$. It is useful to define an equivalent heat transfer constant $\mathbb{h}' = L_o/R_c A$ because $\mathbb{h}'$ can be directly read as the slope constant of the ITC versus temperature plot when both materials are in the normal state. Measurement of the heat transfer coefficient requires a thermal measurement, while that of the electrical specific contact resistance *RcA* could be determined by a (presumably simpler) electrical measurement. Measurement of electrical contact resistance has been important for *semi*conducting integrated circuits, with typically 1 ohm-μm^2 as a minimum attainable value[12,13] and a theoretical minimum of 0.1 ohm-μm^2 for metal/Si.[14] For semi-conductors contact resistance is known to be largely determined by carrier concentration and having a clean semi-conductor surface, along with the work function of the chosen contact metal (reducing the Schottky barrier to an Ohmic contact)[15]. As will be discussed below electrical contact resistance for a normal-metal to superconductor are generally lower, ranging from 1 to 0.001 ohm-μm^2.

Equating the rightmost term in Equation 5 with the righthand side of Equation 4, and rearranging the terms gives a working equation for the interfacial thermal conductance per unit area across the superconductor to normal-metal boundary:

$$\left(R_{th,es}^{BRT}\, A_c^{BRT}\right)^{-1} = {G_{th,es}^{BRT}}/{A_c^{BRT}} = 4\left({k_B^2}/{e^2}\right)\left(\frac{T}{R_c^{BRT} A_c^{BRT}}\right)\left\{F_1(-y) + y\ln(1 + exp(-y)) + \tfrac{1}{2}y^2/(1 + exp(y))\right\}.$$

Equation 6

The Wiedeman-Franz law for interfacial thermal conductance will also be used to consider another electronic heat transfer mechanism acting across the boundary, a mechanism that functions across both the normal-metal/insulator/superconductor (NIS) and the normal/insulator/normal (NIN regimes. Harding, Pippard, and Tomlinson[16] suggested based on electrical (non-thermal) measurements of a Pb-Cu contact prepared in ambient air that this occurred as patches of an oxide forming a tunneling barrier. They considered the total resistance below T_c would be a parallel combination of the NIS tunneling and

clean NS (normal-superconductor) Andreev paths. The clean NS thermal transport is described by Equation 1. To evaluate the NIS heat transport we will use the electrical conductance of a NIS tunnel junction at zero volts bias transforming this into an interfacial thermal conductance using the Wiedemann-Franz law. Giaever and Megerle[17] formulated the NIS tunneling current as an analytical series solution which can be differentiated with respect to bias voltage to provide the electrical conductance. Noting that the electrical conductance $dI_{NIS}/dV = 1/R_{NIS}$ and in the normal state $dI_{NIN}/dV = 1/R_T$ is constant for the conditions under consideration, at zero voltage this series solution becomes

$$\frac{1}{R_{NIS}} = \frac{2}{eR_T}\frac{\Delta}{k_BT}\sum_{m=1}^{\infty}(-1)^{m+1}\, m\, K_1\left(m\frac{\Delta}{k_BT}\right).$$

Equation 7

Where K_1 is the first-order modified Bessel function of the second kind. Using the Wiedemann-Franz law to convert the above electrical resistance into thermal conductance per unit area yields

$$\frac{G_{NIS}}{A_{NIS}} = \frac{L_oT}{R_{NIS}A_{NIS}} = \frac{2\,(\pi^2/3)(k_B^2/e^2)T}{eR_TA_{NIS}}\left[\frac{\Delta}{k_BT}\sum_{m=1}^{\infty}(-1)^{m+1}\, m\, K_1\left(m\frac{\Delta}{k_BT}\right)\right].$$

Equation 8

Equation 8 converges somewhat slowly as the temperature approaches near to T_c, because K_1 grows large due to the gap in the argument going to zero; the term in the square brackets goes to 1, the large values of K_1 being compensated by the small values of the gap in front of the summation. In the plots below this equation will be calculated out to $m = 100$. In the opposite direction, as the temperature becomes small, only the first term in the summation is significant. For large values of Δ/k_BT the NIS thermal interfacial conductance will decay due to the first-order modified Bessel function of the second kind being well approximated as $K_1\left(\frac{\Delta}{k_BT}\right) \approx \sqrt{(\pi\Delta/2k_BT)}\; exp(-\Delta/k_BT)$ when $\Delta/k_BT > 5$.

Both Griffin and Maki's two equations (Equation 2 and Equation 3) and the adapted Giaever and Megerle (Equation 6) describe tunneling through an insulator as the transport mechanism. It is not clear to the present author how these two relate, this must be left to future analysis.

In 1963 Strässler and Wyder[18] proposed a modification of the BRT equation to account for the heat caried by electrons across a superconductor to normal-metal interface. They assumed that all electrons with energies below the gap were totally reflected (this was prior to Andreev's 1964 publication), that the layer thicknesses were periodic and that the mean free path of the electrons was larger than that layer thickness, and that the mean free path could be described as step function where energies below a cut-off were taken as zero, and for the energies above that cut-off were equal to the normal state mean free paths. This cut-off was implemented as a *raising* of the gap energy used in the BRT equation by a factor $(1+\beta)$, which from a fit to data taken on two Indium wires at various magnetic fields resulted in $\beta = 0.172$. Considering the type of samples that will be examined below versus the assumptions made by Strässler and Wyder, their theory is unapplicable. The present analysis will focus on the extended Andreev

(Equation 1), that of Griffin-Maki (Equation 2 and Equation 3), the adapted-BRT (Equation 6), and NIS tunneling (Equation 8).

Andreev, Griffin-Maki at low temperatures, the adapted-BRT, and the NIS equations are all strongly influenced by the multiplicative $\exp\left(-\Delta/k_B T\right)$ term, reflecting the freeze-out of quasi-particles into Cooper pairs as the temperature is lowered.

The interfacial thermal boundary resistance due to lattice vibrations (phonons) for small temperature difference is taken to follow[19] $R_b = B/T^3$ where B is a constant with units of cm^{2}K^4/W and is commonly calculated with either of two models-- the Acoustic Mismatch Model (AMM) or the Diffuse Mismatch Model (DMM). These typically differ in their resulting calculated values for B due to differences in the assumptions of their theoretical derivations, and often as not differ from experimentally measured values[20,21].

Comparing Theory With Experiments

Suitable experimental measurements of dissimilar metal interfacial thermal conductance exist in the literature for Pb-Cu and Sn-Cu covering both superconductor to normal-metal, and normal-metal to normal-metal heat transfer. Figure 1 shows a schematic representation of the method used by Barnes and Dillinger[22], and by Schumann, Nitsche, and Paasch[8]. It is a four temperature sensor technique that, for sufficiently small temperature differences across the materials, allows a linear extrapolation to the interface and temperature jump ΔT_b to be determined.

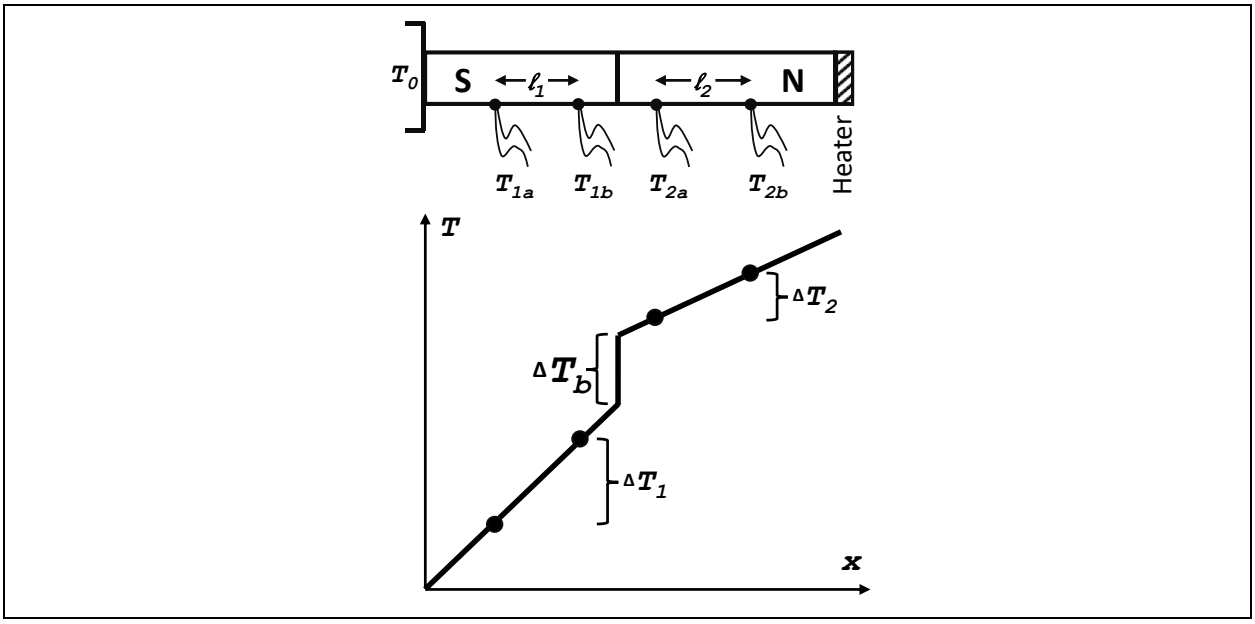


Figure 1 – Schematic of the four temperature sensor method for measuring the interfacial thermal boundary conductance between a superconductor (S) and a normal-metal (N).

Experimental data from the literature can then be fitted to the Andreev, Griffin-Maki, NIS tunnelling, and the adapted BRT equations for temperature ranges where the electronic heat carriers dominate. As

a first example, Schumann et al.[8] prepared a Pb-Cu sample by casting molten Pb under normal atmospheric conditions in a mold on a Cu rod whose mechanically polished surface had been pre-coated with Pb. Their data is plotted in Figure 2. In the normal state (rendered by a magnetic field) the expected linear dependence was found. For the superconducting state on a log-log plot Schumann et al. reported a T^5 dependence for temperatures below $T_c/2$, and shallower slopes above that, clearly this data does not conform to the T^3 expected from AMM or DMM phonon transport theory. The dashed-dotted orange line of Figure 2a is for a DMM pre-factor of 3.14 K^4-cm^2/W, which (not shown on the plot) is not too different from the 2.78 K^4-cm^2/W AMM value given by Schmann et al. The fact that the data's behavior does not follow T^3 does not contradict AMM or DMM theory, rather in the temperature range studied by Schumann et al. the phonon contribution is expected to be only a minor contributor to the ITC. Phonons would only dominate at a normal-metal to superconductor interface below $T_c/5$, a temperature regime unavailable in Schumann et al.'s apparatus. (Also, as will be seen later in the text, the current status of AMM or DMM theory has yet to be refined for "dirty" interfaces.) Other researchers have measured the interfacial thermal conductance at temperatures where the phonons do dominate, and also the transition region $0.2 < T/T_c < 0.3$ where both transport mechanisms are important acting in parallel, and will be examined later.

Taking the T_c of Pb to be 7.2 K and the gap at zero temperature Δ_0 to be $2.15k_BT_c$[23], the superconducting gap is calculated using Sheahen's[24] explicit approximation formula $\Delta = \Delta_0\sqrt{\cos(\pi\,(T/T_c)^2/2)}$ which matches BCS[25] to at most as a 3% overprediction, fortunately, this makes the match closer to the actual gap for Pb as measured by Gasparovic et al.[23], excepting for the region $T > 0.98T_c$ where the formula's over-prection becomes larger on a percentage basis, but consideing the values, since the gap is aprroaching zero the exponential terms in the ITC equaiotns are going to one and do not appreciably alter the the resulting calcuated interfacial themral conductances. The same general agreement between the predicted gap and the experimentally measured gap[26] is true also for Sn. Lastly Pb is known to have two gaps, using the higher gap $2.35k_BT_c$[23,26] imperceptible change in the plotted curves of Figure 2 and only a slight shift in the T/T_c tick mark locations across the top x-axis. If an oxide layer is present, then AMM or DMM calculations for a direct NS junction must be altered to represent the NIS situation. Present theory does not exist for phonons across the very thin insulating layer in an NIS.

The red dotted trace in Figure 2a shows the Andreev interfacial thermal conductance as calculated using Equation 1. However, to align with the experimental data it was necessary to divide the Equation 1 Andreev values by 86.2, which in one light can be viewed as a NS direct contacting area reduction to 1.12% of the actual cross sectional area interface of the Pb-Cu rod. If only ~1% of the contact area is participating in Andreev thermal transport, this suggests that ~99% of the contact is somehow insulating. As mentioned earlier, Harding, et al. suggested that this occurred as non-perfectly metallic patches of an oxide forming a tunneling barrier. They also determined that Pb-Cu interfaces formed using a sputter ion bombardment pre-clean followed by an *in-vacuo* deposition of the Pb could form clean NS contacts, or as an alternative use of a solder flux under normal conditions could also form clean NS contacts. Schumann et al.'s pre-application of the Pb to the polished Cu surface under ambient conditions would be consistent with having a mostly "unclean" contact. Examining the scaled Andreev curve, originally derived by Andreev only for

temperatures below $T_c/2$ it is amazing how well the extended and scaled version of Equation 1 fits the data.

While the thermal conductance experiments examined in Figure 2 through Figure 9 use a single temperature for each data point, the experimentalists involved used small heat currents to creates small temperature differences, such that a single average temperature is an acceptable value. However it is worth discussing thermo-electric effects that can occur when a heat current passes across a superconductor and normal-metal interface. Excess electrical resistance in an open-circuit can be measured when an imposed heat current creates a charge imbalance Q* whereby quasi-particles go into the superconductor and are compensated by a Cooper pair current in the opposite direction to maintain a zero total current. Harding et al.[16] in a non-thermal experiment measured the excess resistance for ion bombardment cleaned *in-vacuo* deposited Pb onto Cu to be 0.0015 Ω-μm^2. They found that less well cleaned interfaces, particularly those formed in ambient air, could be as large as 0.185 Ω-μm^2. Van Harlington[27] did impose a heat current measuring at T_c about 1 nΩ worth of excess resistance on a 3 mm diameter Pb-Cu interface (0.0071 Ω-μm^2), and using the theory of Hsiang and Clarke[28] calculated an effective charge imbalance thickness of 2.7 μm. (It should be noted that Van Harlington applied the Pb to the Cu in ordinary air, so it is unknown just how much truly clean NS contacting area was present. This might have been extractable as was done in Figure 2 but the heating powers were not reported.)

This excess electrical resistance is significant for clean NS contacts typically in the range $0.9 < T/T_c < 1$ with its maximal value near or at T_c and fading to zero as the temperature decreases. The above-mentioned work by Hsiang and Clarke indicates that it goes to the normal state electrical resistance of the superconducting material for the effective charge imbalance length. While this would appear to bridge the region not covered by Andreev, it is important to note that the excess resistance increases as the temperature increases, which would show up as a reduced thermal conductance while approaching T_c. In the region near T_c the projected linear fit to the normal state data in Figure 2 is indeed above that of both the scaled Andreev and adapted BRT curves. Unfortunately Schumann et al.'s Pb-Cu data only goes up to $0.86T_c$ so does not help resolve whether thermo-electric effects are discernable in the thermal interfacial conductance.

Taking the adapted BRT equation and performing a least-squares fit to Schumann et al.'s Pb-Cu data gives an *RcA* of 0.0771 ohm-μm^2 which goes very nicely through the data points. Schumann et al. also applied a magnetic field and measured the ITC between normal-Pb and Cu and approximate in value to the 0.0455 Ω-μm^2 derived from the normal-state slope of 56.645 W/cm^{2}K^2 using $\mathbb{h}' = L_o/R_cA$. The adapted BRT line falls below the projected normal state by 1.7x at T_c. When we later examine the data of Challis and Cheeke[7,29] it will be seen that the extrapolated normal state interfacial thermal conductance can also instead fall below the adapted BRT values. When both metals are in the normal state the thermal resistance is quite low so we might speculate that combined extrapolated and experimental error may be large above T_c. However if we do consider the projected normal state line to be good above T_c then fitting Equation 6 using a specific contact resistance of 0.0455 Ω-μm^2 results in the thin dashed blue line of Figure 2a which matches exactly with the projected normal state above T_c, but below T_c runs significantly above the data.

Fitting the low temperature Griffin-Maki expression (Equation 2) through Schumann et al.'s lowest temperature data point yields an RnA = 0.546 Ω-μm^2 shown as the purple lozenged curve in Figure 2b but does not fit to the rest of the data as well as the scaled Andreev equation nor the adapted BRT. Fitting the high temperature Griffin-Maki expression (Equation 3) through Schumann et al.'s highest data point results in a different RnA = 0.117 Ω-μm^2 and deviates from the subsequent lower temperature data. Using the low temperature RnA would only shift the curve downwards, taking the trace further in disagreement with the data. Fitting to the extrapolated normal state line would shift the trace further upwards and not agree with the $T < T_c$ data. It is tempting to consider the Griffin-Maki high temperature expression in parallel with the scaled Andreev to bridge the region near T_c where the Andreev falls away, but it is not clear by what mechanism the Griffin-Maki heat flow would then disappear when the scaled Andreev takes over at colder temperatures than the near T_c.

It is reasonable to take a scaled Andreev heat flow to act in parallel with NIS tunneling, which is shown in Figure 2c. The solid purple line is the NIS thermal conductance calculated using Equation 8 again using a specific tunneling resistance R_TA of 0.0455 Ω-μm^2. The dotted green curve is the sum of the two contributions, determined by a least-squares fit to the data. This required the rescaling of the extended Andreev equation by a factor of 1/164. A new feature becomes visible as a bump just below T_c, indicated by an arrow in the upper right. Also note that the y-axis of Figure 2c covers only three orders of magnitude, this to make it easier for the reader to see on the expanded scale. The peak conductance is 1.24x that of the conductance at T_c. Although this peak may be an artifact of the summing of the two equations, there is evidence from the electrical (non-thermal) experiments of a dip in electrical resistance just below T_c which would correspond to a peak in interfacial thermal resistance. The electrical measurements of Harding et al.[16] an excess resistance for ion bombardment cleaned *in-vacuo* deposited Pb onto Cu to be a quite small value of 0.0015 Ω-μm^2. Other samples, prepared in an air ambient, were measured to be for example as large as 0.117 Ω-μm^2, which dropped in resistance0.102 Ω-μm^2 at $0.95T_c$, and then would rise back up to 0.185 Ω-μm^2 at $0.27T_c$. Harding et al. attributed the drop in specific electrical resistance to NIS tunneling operating in parallel with a small ~1% area of clean NS Andreev tunneling transport. Hence the peak observed in the theoretical sum curve of Figure 2c is plausible. Other researchers have also found this dip to a brief minimum in electrical resistance just below T_c. Harding et al. suggested that the similar dip in the Pb-Ir-Pb sandwich samples of Clarke et al.[30] were presumably not free from contamination. Hsiang and Clarke[28] observed an electrical resistance minimum at $0.75T_c$ in their Pb-Cu sample attributing this, like Harding et al., to an oxide layer forming an NIS junction. Schumann et al.'s apparatus could not resolve interfacial thermal conductance values that close to lead's $T_c$and it will remain for future studies to look for such a peak.

It could also be possible that both BRT scattering and NIS tunneling mechanism are occurring in the same sample. Figure 2d shows this assuming that the two operate as thermal resistances in parallel. (The conductance would simply sum.) Taking that their combined ITC must align with the projected normal state and least-squares fitting the data produces R_TA=0.0734 Ω-μm^2 for the NIS contribution and for the a-BRT an R_cA=0.120 Ω-μm^2. NIS is a larger contributor to the ITC near T_c, but BRT is larger below $0.7T_c$. Although the difference in the fits in (a) and those in (d) are subtle, that of the combined NIS and BRT does look somewhat better and works both below and above T_c.

Given that the NIS mechanism occurs at the actual interface, but that the BRT scattering could be happening in a small thickness layer next to the interface, it is also possible that these two mechanisms sum like thermal resistance in series (the conductance sums as 1/G). Although not shown, this would place the individual BRT and NIS curve above the data, so again taking the sum of the two resistances set to be the normal state slope and performing a least-square fit on the sum produces a specific resistance for NIS tunneling of R_TA=0.0123 Ω-μm² and for BRT R_cA=0.0332 Ω-μm². There seems to be no way of knowing from the thermal data whether the NIS and BRT are in series or parallel.

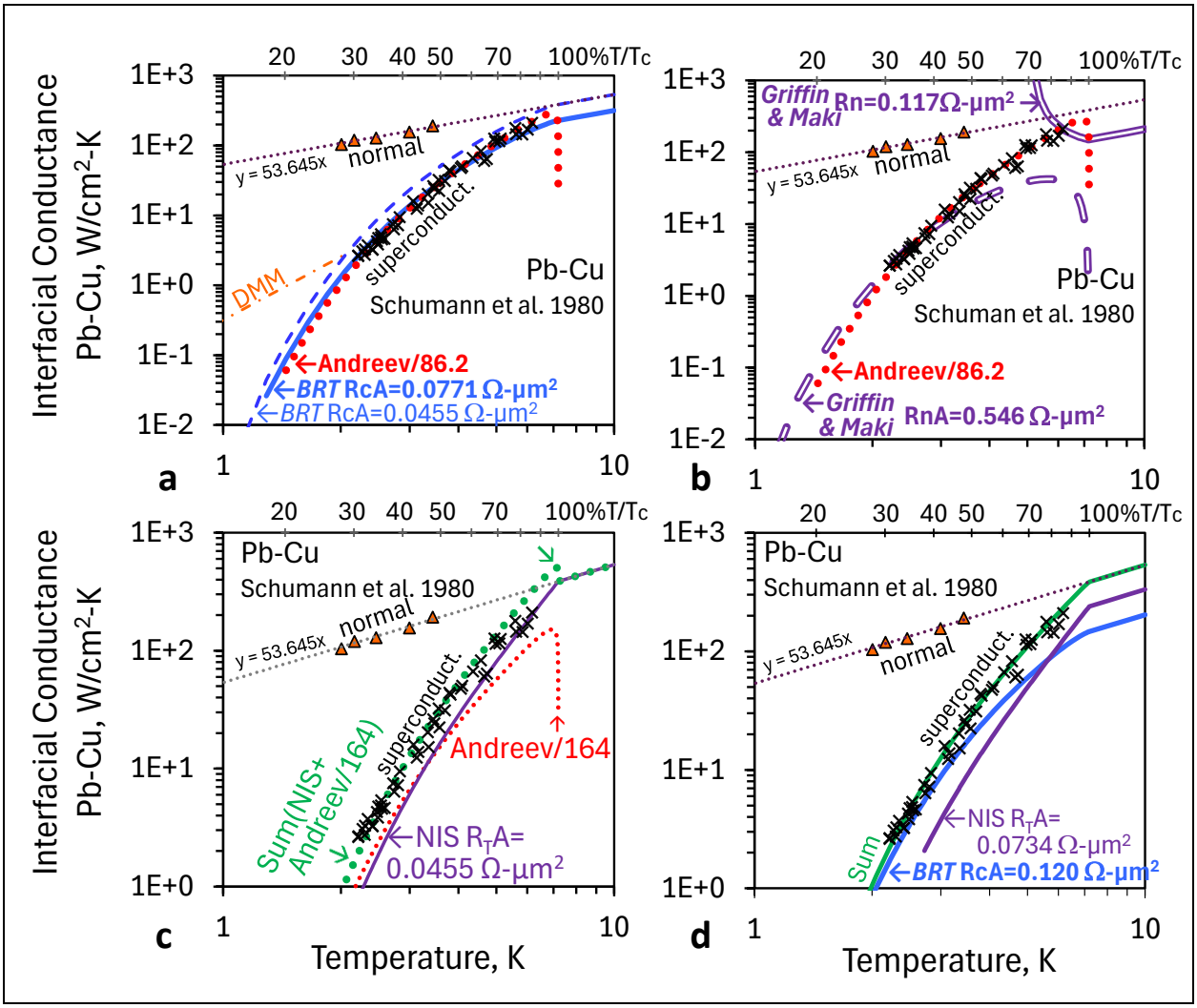


Figure 2 – The experimental data of Schuman et al.[8] for a Pb-Cu interface compared (a) to the DMM interfacial phonon transport (orange dashes), Andreev (Equation 1, red dotted) but scaled by a 1/86.2 factor, , and an adapted BRT (Equation 6, solid blue) with a single contact resistance of 0.0771 Ω-μm² covering the entire range of plotted temperatures or (thin dashed blue) using a contact resistance of 0.0455 Ω-μm² to align with the extrapolated normal state ITC. (b) Griffin-Maki (Equation 2 and Equation 3, purple lozenges) using a large 0.545 Ω-μm² RnA for the low temperature regime and a smaller 0.117 Ω-μm² for the high temperature. (c) Combined parallel scaled Andreev and NIS tunneling (Equation 8) again aligned to the extrapolated normal state ITC. (d) Combined parallel adapted BRT and NIS tunneling.

Schumann et al.[8] also examined a tin-copper interface prepared by casting molten Sn onto a Cu rod. Barnes and Dillinger[31] had earlier also cast molten Sn onto a Cu rod and noted a very dilute alloy zone 0.1-0.2 mm deep in the Sn, attributed to the fact that although slow, Cu can dissolve into the Sn, and thus the interface was not sharp. By contrast Cu has less of a propensity to dissolve into molten Pb, and unlike Cu with Sn, Cu and Pb form no intermetallic compounds[32]. Proceeding nonetheless with the analysis fits to a scaled Andreev and an adapted BRT are shown in Figure 3a. Since the temperature goes from the fully normal state downwards in temperature into the superconducting and no anomalous increase in thermal interfacial conductance is observed the Griffin-Maki equation is not shown, indeed the data suggests the opposite with a slight decrease when transitioning down through T_c. For clarity future plots will not include Griffin-Maki fittings. With regard to the Andreev fit the red dotted curve does go nicely through the data if divided by 289 (equivalent to a ~0.3% NS contact area). Again Andreev cannot extend fully to T_c and beyond into the normal region. Schumann et al.'s data above T_c (small black x's) exhibits linear behavior consistent with a Wiedemann-Franz law for interfacial thermal conductance between two metals in the normal state. Two different fits of the adapted BRT equation are possible, the first being based on the slope of the fully normal region (dashed blue trace), and the second based on fitting to the five data point (larger purple X's) in the solely superconducting region (thin solid blue trace). The derived R_cA products are slightly different, 0.187 and 0.206 ohm-μm^2 respectively. The normal data fit when extended down into the superconducting region is seen in the zoom-in near T_c plot to be slightly above the five superconducting data points, while the fit to the superconducting data points falls noticeably below the normal region data.

Figure 3c shows combined NIS and Andreev tunneling mechanisms. The scaling factor for the Andreev requires division by 1700, implying very little clean NS contact. Again a peak in the summed mechanisms is predicted, regretfully the data is too sparse in this region to determine whether this is real or not.

Figure 3d considers the combined NIS and BRT mechanisms, here summed with the thermal resistances in series to illustrate that the individual curves will sit above the data, but summed to fit the normal state slope. Since it is possible that the Cu has dissolved in the near interface region, summing the thermal resistances in series is conceivably likely. The kinks in the curves at the 3.75 K T_c are off-scale in the main plot; the inset shows these, which occur at 197 and 66 W/cm^2-K for the NIS and BRT respectively. As was observed in Schumann et al.'s Pb-Cu data the best fit to the Sn-Cu data is when the BRT and NIS mechanisms are combined.

Being summed as series thermal resistances, the larger BRT mechanism dominates in the range of the data. The two mechanisms calculate to cross at about 1.6 K, and although not readily visible, for colder temperatures the NIS mechanism is the larger thermal resistance. It should be noted that by 1.6 K ($0.22T_c$ the phonon conductance should be included since the heat carrying elections are largely frozen out into Cooper pairs and decreasing in their ability to transport heat. Again Schumann's et al. apparatus could not be expected to provide data in that regime.

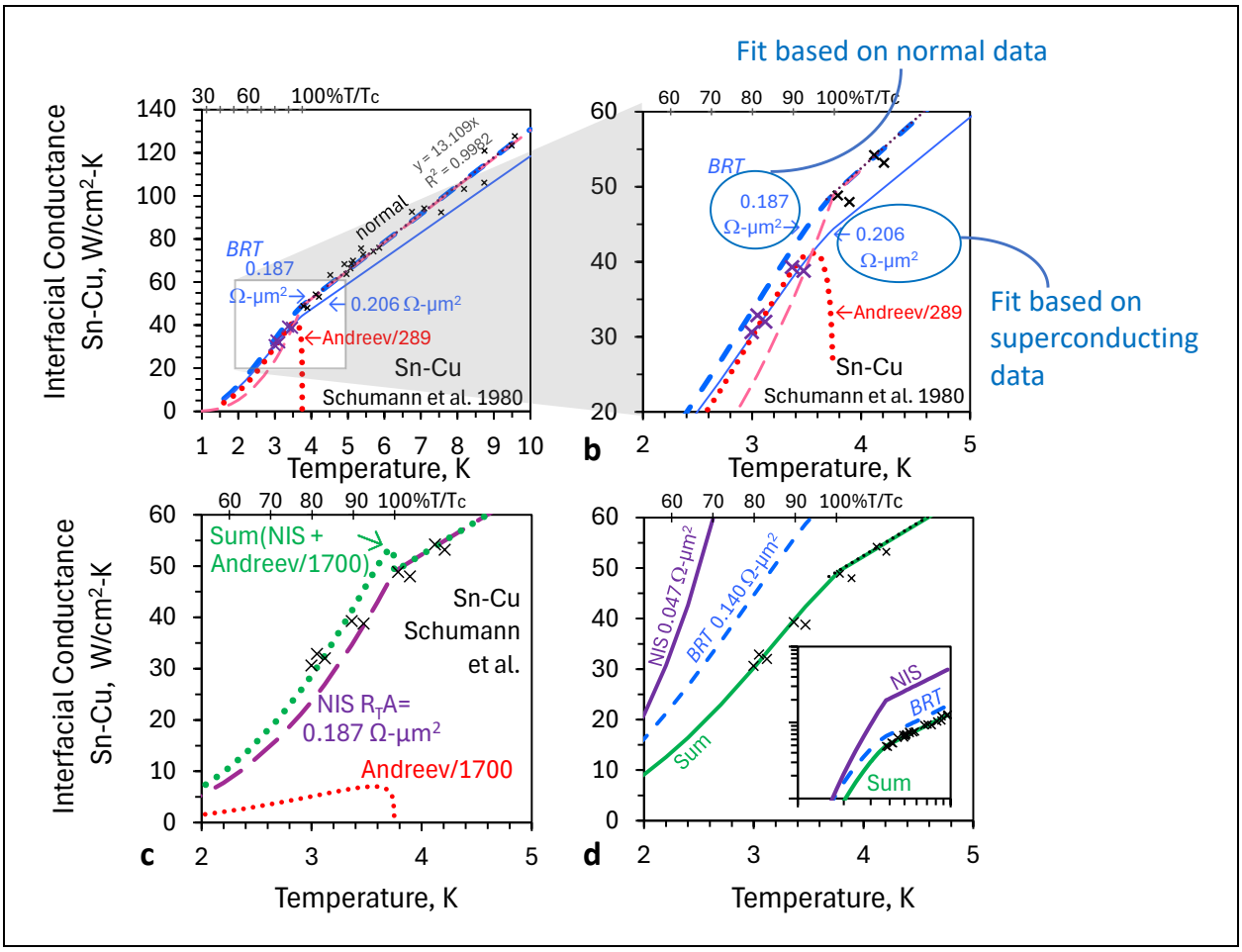


Figure 3 – (a) The experimental data of Schuman et al.[8] for a Sn-Cu interface compared to Andreev (Equation 1, red dotted) but reduced by a 1/289 factor, and an adapted BRT (Equation 6, dashed blue and solid blue) with two different fits: the dashed blue trace uses the data's slope above T_c for the fit, while the thin blue trace uses the five data points below T_c to determine the fit. (b) Zoom in view near T_c. (c) Fits combining scaled Andreev and NIS (Equation 8, dashed purple), and their sum (dotted green). (d) *Series combination* of the BRT and NIS ITC. The inset shows the full dataset in log-log axes spanning 1-10 K and 10-1000 W/cm^2-K.

Schumann et al.'s[8] third experimental test measured the ITC between tungsten and copper but the coldest temperature attainable was 2.6 K and the sample remained normal. They did find a peak in the ITC at ~13 K, and for T < 10 K found that the ITC became linear, consistent with interfacial Wiedemann-Franz behavior with their reported $\mathbb{h}'$=135 W/cm^{2}K^2, equivalent to R_cA = 0.0181 Ω-μm^2.

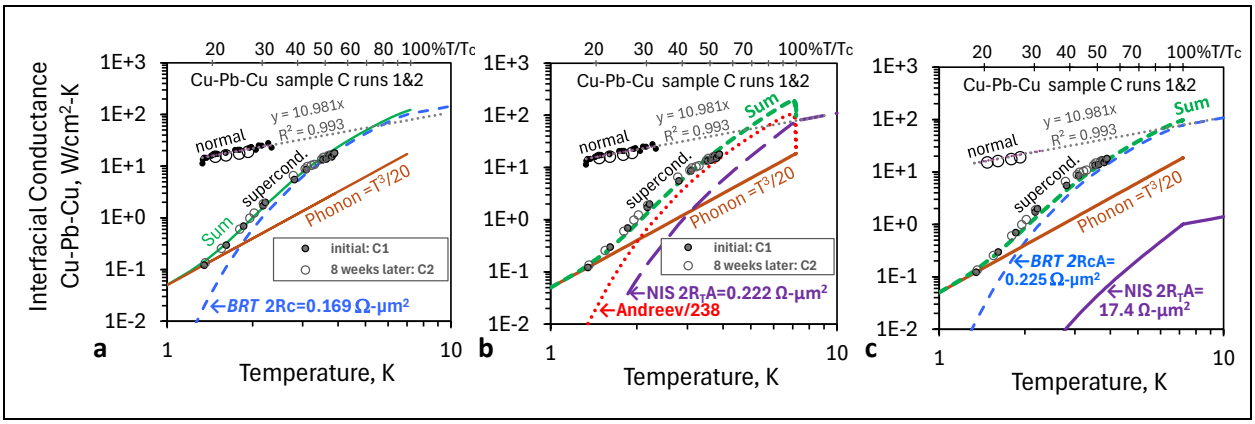


Figure 4 – The interfacial conductance as measured by Challis and Cheeke[7,29] for two Cu disks soldered together by Pb. (a) The solid green curve is the adapted-BRT added to the phonon contribution (b) The dark green dashed trace shows the sum of the scaled Andreev, NIS, and phonon components. (c) The dashed green trace is the sum of the adapted-BRT, NIS, and phonon contributions. The phonon contribution in all three plots has been arbitrarily cut-off from inclusion in the sums above T_c.

The experiments of Schumann et al. did not contain data at low enough temperatures to allow for an analysis of the phonon transport of heat across their interfaces. Seeking other data that might exhibit a discernable phonon component, we next will examine the 1960s Challis and Cheeke[7,29] experiments that measured the interfacial thermal conductance of superconducting and normal 99.995% pure Pb with Cu. Their configuration was not the single interface sketched in Figure 1 but rather that of a sandwich consisting of two Cu disks 0.24 cm in diameter of unstated thickness, soldered together by the Pb and placing the temperature measurements taps as close to the Pb interface as possible. Their best results were obtained with their third experiment denoted as sample C, which had 0.02 cm of Pb between the Cu. They contended that most of the thermal resistance was due to contact resistance. To quantify Challis and Cheeke's claim we may compute the Kapitza length (thermal conductivity divided by the interfacial thermal conductance, K/G)[33] and use the thermal conductivity of superconducting and normal 99.99% pure polycrystalline Pb as measured by Montgomery[34]. At 2 K in the superconducting state this length is (1.42 W/cm-K divided by 1.2 W/cm^2-K) = 1.18 cm. Since this Kapitza length is much larger than the 0.02 cm thickness of the Pb layer we may conclude that the interfacial thermal conductance dominates. In the normal state again at 2 K the Kapitza length is 0.291 cm so again the ITC dominates. In terms of temperature jump the worst case is at the highest temperature tested by Challis and Cheeke: at 3.9 K the bulk conductivity would account for <19% of the temperature drop, rapidly falling to <10% at 3.2 K. In the region of particular interest in Figure 4 from 2.8 K to 1.4 K where the phonon and electron contributions are of the same order, this is estimated to fall from 6% down to <1%. The error being small on a log plot the data shown in Figure 4 and subsequently in Figure 5 and Figure 6 do not attempt to subtract out the bulk contribution, and also the fitted scaled Andreev and fitted adapted BRT do not compensate for the bulk.

Sample C's ITC is shown in Figure 4 where the results are per unit area of one interface face. In the temperature range of 1-4 K studied, the dominant phonon wavelengths would be a few tens of nanometers but the mean free path length for phonons in bulk superconducting Pb can be much larger, in the order of 1 millimeter and typically limited by the sample diameter[35] and hence considerably larger than the thickness of the Pb layer, hence boundary scattering dominated in the bulk. The situation is different for electrons. Wawro[36] determined the mean free path for electrons in Pb just above T_c, for bulk material this comes to 154 nm, three orders of magnitude smaller than the Pb thickness used in Challis and Cheeke's sample C. For electronic transport of heat we can view sample C as being two

interfaces in series, while for the phonons the conductance across the two interfaces could be treated as some mean reflection coefficient at this layer. It is worth noting the Challis and Cheeke made two measurement runs on their sample C separated by 8 weeks, with excellent agreement between the two data sets. For the superconducting tests they state that they were expecting the interfacial thermal conductance to go as T^3 but instead found it more like $T^{5.7}$ for $T < 2.5\ K$ ($T < 0.35T_c$).

Further analyzing Challis and Cheeke's sample C data, if we assume the phonons largely dominate below $0.2T_c$ and fit their coldest data points according to a proportionality to T^3 we find that the ITC is equal to $T^3/20$ (the brown line in Figure 4). Recall that for a single Pb-Cu interface the DMM 3.14 K^3cm^2/W, so the fitted value of B=20 K^3cm^2/W is considerably larger than even twice the DMM

Applying Equation 6 for the adapted BRT (with 2RcA=0.156 Ω-μm^2 or for this case $\mathbb{h}' = L_o/2R_cA =$ 15.6 W/cm^2-K^2) to the data gives the dashed blue trace. The sum of the phonon and adapted BRT are shown as the green trace and is seen to go through all data points, especially in the region from 1.4 K to 2.8 K ($0.19T_c < T < 0.39T_c$). Above T_c the phonon contribution is arbitrarily omitted but being already 1 order of magnitude below the projected ITC the phonon contribution would add only a small amount to the ITC prediction. The phonon transport in the presence of a large concentration of electrons is beyond the scope of this present paper. Nonetheless it is observed that the adapted BRT is slightly above the projected normal state above T_c, which was measured by applying a magnetic field, which fits very well to T^1 and when extrapolated out to T_c would indicate an ITC of 79 W/cm^2-K while the sum of the phonon plus adapted BRT (the green curve) at T_c is predicting 113 W/cm^2-K, a 1.43x factor different. This is in the opposite direction from Schumann et al.'s Figure 2 Pb-Cu normal state extrapolation which was seen to be 1.7x greater than the adapted BRT at T_c.

A key feature of Figure 4a is the observed triangular region formed between $0.2T_c$ and $0.5T_c$ where heat transport changes from phonon dominated to electron dominated, with the two curves crossing for equal importance at 1.7 K. It takes the sum of the two contribution mechanisms to match with the data.

Utilizing Challis and Cheeke's sample C normal state slope $\mathbb{h}'$ =10.98 W/cm^2-K^2 and the Lorenz number we can find that this is equivalent to an electrical contact resistance 2RcA=0.222 ohm-μm^2. While this would allow the blue dashed trace of Figure 4a to coincide exactly with the extrapolated normal state ITC above T_c it causes the adapted BRT to slightly underpredict the data (not shown), the green sum curve would go through the bottom of the data points for temperatures of above 1.8 K. Adjusting the phonon contribution next to be T^3/12 can move the sum curve back through the center of those points but renders the sum curve to overpredict the ITC by 2x at Challis and Cheeke's coldest data point.

Applying Equation 1 to consider Andreev thermal conductance (based on the area of a single interface) and summing this with the NIS taken to align with the projected normal state and the phonon line results in the dark green dashed curve which is the least squares fit to the data (Figure 4b). Note that the Andreev component (red dotted curve) must be divided by 238 (or for two identical single interfaces in series $G_{th,es}^{A",tot}/238 = 1/238R_{th,es}^{A",tot} = \left(238\left(R_{th,es}^{A",ssingle} + R_{th,es}^{A",single}\right)\right)^{-1} = \left(476R_{th,es}^{A",single}\right)^{-1}$ since resistances add in series) to permit the summation trace to align with the data. At higher temperatures the summed dark green dotted trace is above the data and above the projected normal state, while below 3 K it falls a bit below the data.

Figure 4c considers the sum of the adapted-BRT, NIS, and phonon contributions. While this enforces that the trace above T_c aligns with the projected normal state, the fit to the actual data is not quite as good as using the adapted BRT and phonon contributions seen in Figure 4a. Comparing the conductances it is seen that the NIS contribution to the ITC is two orders of magnitude below the adapted BRT. The transport of heat across the interfaces of sample C appear to be dominated by defect or impurity scattering above $0.5T_c$, and by phonons below $0.2T_c$.

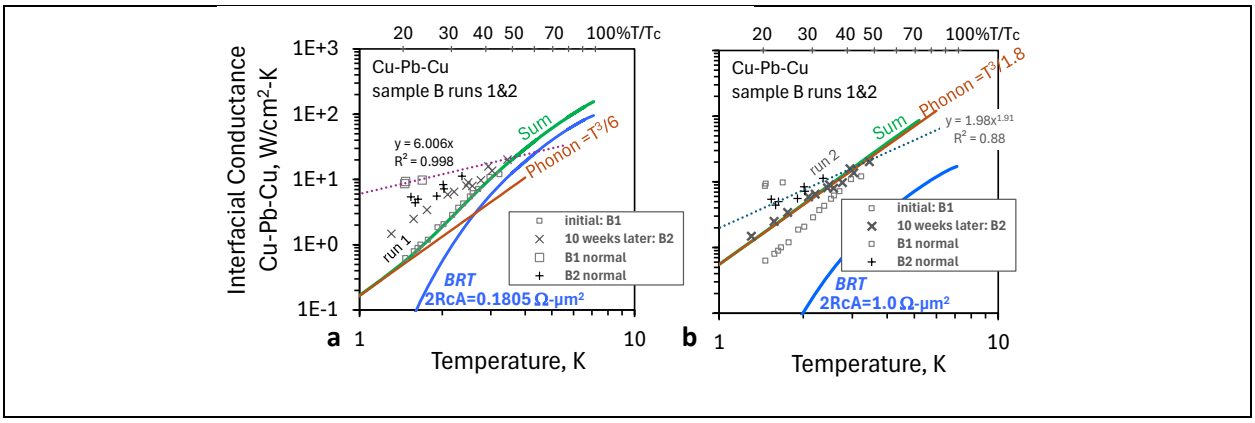


Figure 5 – Fit to Challis and Cheeke's sample B, with (a) the initial test run, and (b) 10 weeks later.

Prior to sample C Challis and Cheeke prepared sample B using the same size Cu as in sample C, but sample B had a thinner Pb layers of 0.008 cm. The contribution of the temperature drop across the thickness of the Pb is estimated to be less than 5% for run B1 at 3.2 K, dropping to <1% below 2 K. Challis and Cheeke considered the first run on sample B to exhibit a $T^{4.1}$ behavior and could not explain why it differed from the expected T^3 of phonon transport. Instead, if we set the phonon component to $T^3/6$ to largely account for the coldest temperature points in Figure 5a the combined adapted BRT plus the phonon results in the sum (green line) going through all of the run 1 data points over the entire range of temperatures tested. (A scaled Andreev curve is not shown here but as seen earlier it can also explain the data when combined with the phonon component over the short span of this data.) Using $T^3/6$ might suggest that this could be considered to be two DMM resistances in series, namely 3.14 + 3.14 ≈ 6 (K^4cm^2/W) but this is probably a coincidence. Challis and Cheeke took only three data points in the normal state, which all sit an order of magnitude greater for the ITC than the superconducting state. Extrapolating a T^1 fit has the green sum curve being 2.25x larger than the normal state at T_c. An attempt was made to fit to a combination pf BRT, NIS, and phonon contributions (not shown), but adding even a small amount of NIS degraded the fit. Attempts to make a fit using just the NIS as determined by the slope of the normal state of run B1 plus the phonon contribution (not shown) resulted in a sum that clearly did not align with the data; at 3.23 K the prediction was just 64% of experiment.

Additionally, sample B's soldered interfaces were apparently not stable because in a measurement conducted 10 weeks later (Figure 5b) the interfacial thermal conductance actually becomes larger. Challis and Cheeke found the new ITC to go as $T^{2.8}$ and concluded that the interface was phonon dominated but gave no speculation as to what changed in the sample to cause this. Using our new analysis technique it would appear that run 2 of sample B is 3.3x more transparent to heat carried by the phonons and 5.5x more thermally resistant to heat carried across the interface by electrons. An increased electrical contact resistance would be consistent with oxide formation, and the approximately T^2 power law fit to the normal state ITC of B2 suggests an amorphous layer in the thermal path, it being known that at low temperatures the thermal conductivity for amorphous solids goes nearly as the square of the temperature.[37] Another clue could be in the surface preparation. The authors state that their Pb to Cu soldering was done with an acid flux (Bakers fluid) but only sample C was electrolytically polished beforehand to remove surface damage, while samples B and A were merely as-machined. Contrary to this sample A did exhibit unchanging ITC values when measured a second time 10 days later, but as will be discussed below, sample A's aggregate performance across its multiple Pb solder layers was likely internally inconsistent. For all this, the true cause for the change in sample B remains a mystery.

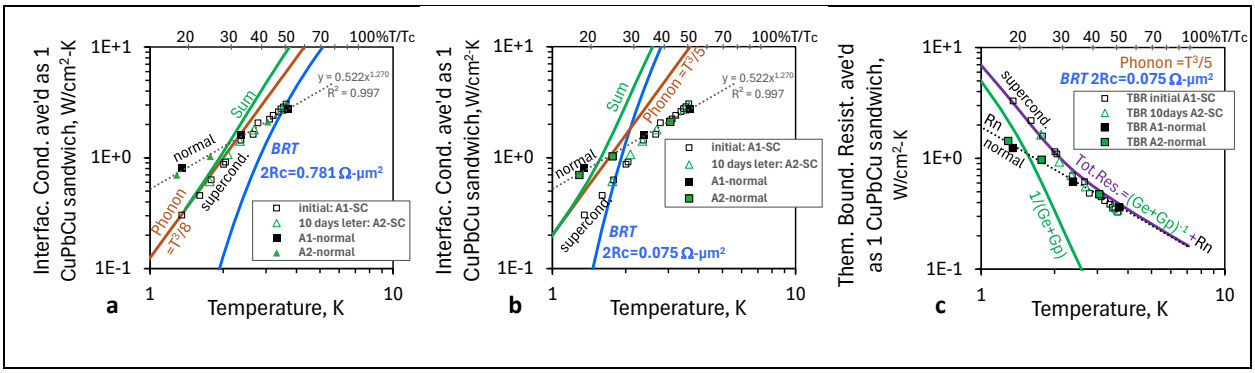


Figure 6 – Analysis of Challis and Cheeke's[7,29] multi-layer sample A. Open symbols are superconducting state and filled symbols normal. (a) simple-minded application of phonon and electron thermal carrier fittings, (b) corrected phonon and electron fittings, (c) adding the normal-state thermal resistance due to the copper disks as a series resistance to the paralleled phonon and electron transport (green) showing as the purple curve the total resistance aligning with the entire data range.

Figure 6 shows data from Challis and Cheeke's sample A. Unlike B and C, sample A consisted of 12 Cu disks with 11 Pb layers forming 22 interfaces and the reported ITC in the figure averaged to one sandwich. Data taken 10 days later was consistent in both the superconducting and normal states. The authors did state that the preparation of the multiple sandwich sample was more difficult than the single ones, and that the lower than expected ITC could be due to the contact areas being less than the full cross section. Runs 1 and 2 in the superconducting state for sample A were found to produce the same ITC and fitted well to T^3 only at temperatures below 2 K where phonon dominance would be expected. However at higher temperatures and unlike samples B and C, the ITC decreased below that of T^3. Applying the analysis developed in the present paper, Figure 6 shows a T^3 fitting through the lowest temperature data point (brown line) and the adapted BRT through the highest (blue). The sum curve (green) clearly does not fit this data. A telltale to the behavior in sample A can be seen in the applied magnetic field normal-state data, where above 3 K (42% the T_c of Pb) the ITC takes on the $T^{1.2}$ of the normal state, close to the expected $T^{n=1}$ form of a normal-metal. While the heat transfer across the interfaces in the superconducting state is the sum of the phonon and electron conductances (parallel conductances add), each interface in this stack is resistively in series with the bulk copper of the disks. In the normal-state both the copper's bulk thermal conductivity and normal-state interfacial thermal conductance are expected to follow the Wiedemann-Franz Law so it is difficult to separate out the two from the normal-state data; however we can examine a limiting case where all of the extra resistance is due to the bulk copper's thickness. From sample A's dimensions this would imply that the copper's thermal conductivity [W/cm-K] is approximately $= 0.063\ T^1$, which combined with that copper's thermal conductivity at low temperatures is linearly related to its Residual Resistivity Ratio (RRR) as $= RRR\ 0.01566\ T^1$ (fitted from the low temperature linear portion of Hust and Lankford[38]) results in a RRR of 4.01. This is a very low RRR for copper, for comparison Oxygen Free High Conductivity (OFHC) copper is 99.99% pure and has been found to typically have a RRR between 50 and 100[39] and Challis and Cheeke state that they used an order of magnitude more pure (99.999%) copper so we might expect a higher RRR than 4. This does imply that there is something wrong with the interfaces.

Subtracting out the normal-state ITC and re-applying fits through the lowest and highest temperature points in the superconducting state ITCs for phonons and electrons respectively results in Figure 6b where again the conductances are in parallel and sum to the green curve. The green curve is dominated by the phonon interfacial component (brown curve) at the lowest temperatures. The electron component's contact resistance of 2RcA=0.075 Ω-μm^2 is smaller than most of the other contact resistances examined so far but would really only become noticeable at temperatures above 3 K where it is swamped by whatever is wrong with the interfaces as indicated by the normal-state measurement. To account for the apparent total thermal boundary resistance, the normal-state resistance is then added to the summed superconducting ITCs as resistance (inverse of the conductance sum) and shown in Figure 6c. Here the resistances add in series, namely the solid green and black dashed curves add together to produce the purple curve, which nicely goes through all of the superconducting data. While this analysis has been able to isolate the phonon and electron components of the ITC, it does not indicate just what is defective with the muti-layer stack's structure.

Looking back, their sample B might be analyzed as just shown for the multi-layer stack sample A, but sample B was a single sandwich, and without knowing just where the thermometer taps are located this is not possible.

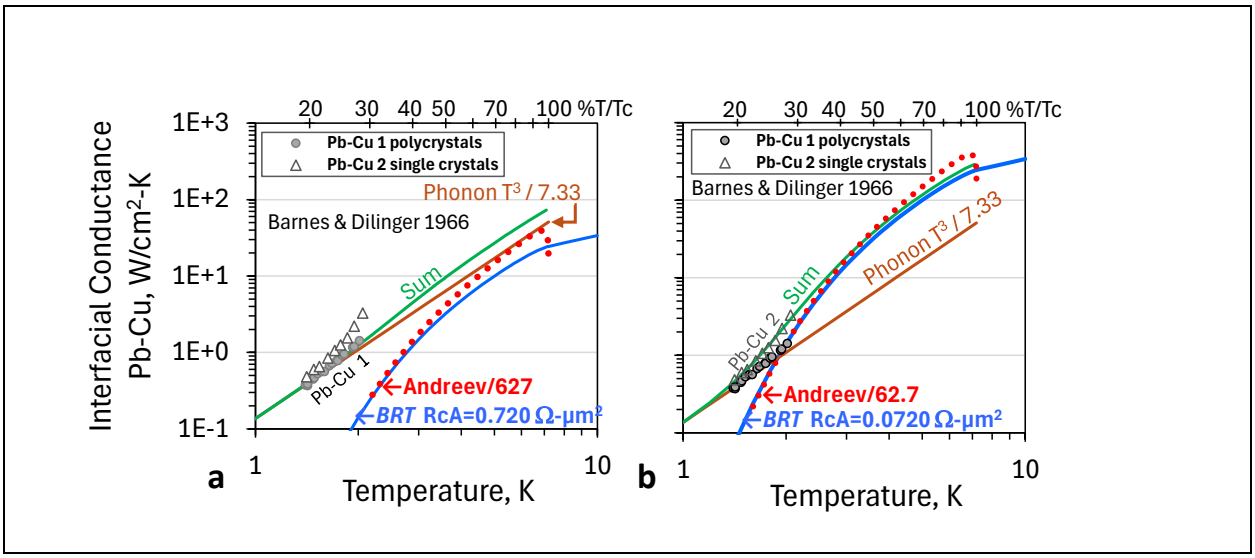


Figure 7 – Interfacial Thermal Conductance data form Barnes and Dillinger[31] and fits for (a) polycrystalline Pb to polycrystalline Cu, and (b) fits for the single crystal Pb to single crystal Cu.

Also in the 1960s Barnes and Dillinger[22,31] studied Pb-Cu and Sn-Cu single interfaces using the four temperature sensor method by casting the molten Pb or Sn onto a Cu rod. The temperature range in their apparatus was limited to at best a narrow 1.4 K to 2.1 K range (18%-0.29% of T_c for Pb; 35%-56% of T_c for Sn). Their Pb data is particularly interesting as the lowest temperature data point will be in the phonon dominated regime allowing a T^3 fit and the highest temperature to be in the regime where both phonon and electron transport are important. Their sparse normal-state data for the interfacial thermal resistance of the Pb-Cu samples showed that the interfaces became very conductive (very close to zero in their apparatus) and as such too noisy to permit any sort of accurate or reasonable fit to a $T^{n=1}$ behavior.

Figure 7 shows the superconducting data and our fits to their sample Pb-Cu1 (polycrystalline Pb on polycrystalline Cu) and Pb-Cu2 (single crystal Pb on single crystal Cu.) Phonon transport is important over the entire temperature range of the data sets, being dominant for sample Pb-Cu1 and approximately of the same order of magnitude to the electronic in sample Pb-Cu2. Both phonon fits for these two different samples use $T^3/7.33$ but have very different electronic components, with the polycrystalline sample PbCu1 having a large contact resistance of R_cA=0.720 Ω-μm^2, exactly a factor of 10x larger than the 0.0720 Ω-μm^2 of the single crystal PbCu2. The Andreev scaling also goes by this exact 10x. If Andreev is the electronic heat transport mechanism then it could be inferred that the actual NS contact area is merely 0.16% of the cross section in Pb-Cu1, and 1.6% in Pb-Cu2. An NIS fit could be performed but the normal-state data being unusable this is not shown; presumably it will be similar to the a-BRT and scaled Andreev in the range of the data. The electron contribution to the ITC for the single crystalline Pb to single crystalline Cu is 10x larger than the polycrystalline. Whether this is due to the crystallographic orientation or merely a coincidence of the sample preparation cannot be determined.

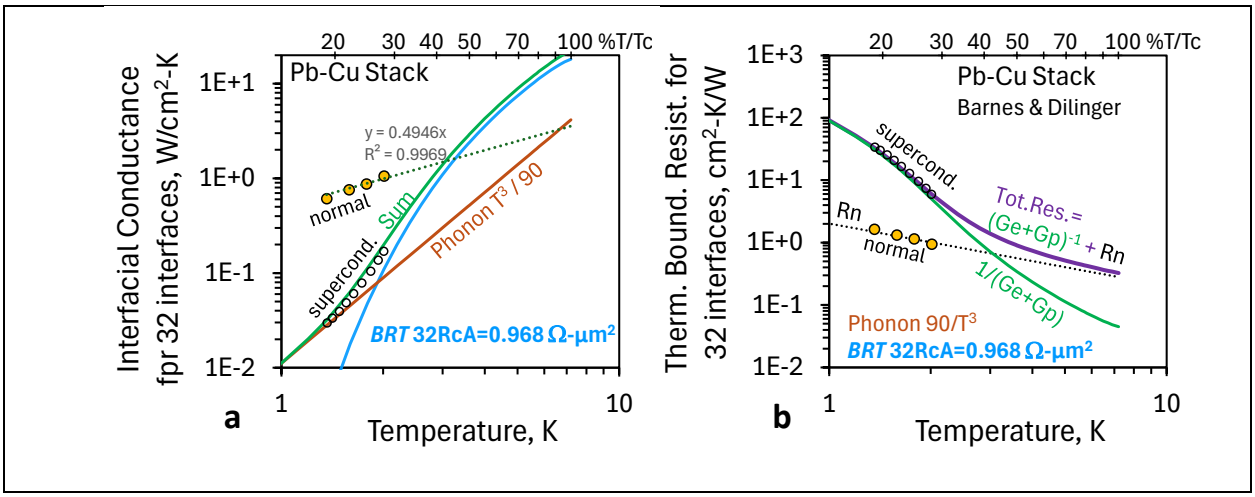


Figure 8 – (a) Interfacial Thermal Conductance data converted form Barnes and Dillinger[31] thermal conductivity measurements on a multi-layer stack of Cu disks with Pb solder The fits have subtracted the normal state contribution. (b) Thermal boundary resistance, with the purple curve showing the addition of the normal state with the paralleled sum of the electrons and phonons.

Barnes and Dillinger also prepared a multi-layer stack of OFHC Cu disks soldered together with Pb and reported its effective thermal conductivity in both the superconducting and normal states. The normal state fits well to K=2.71 T^1 with the thermal conductivity K in W/cm-K. Using the physical dimensions given by Barnes and Dillinger and the previously used relationship between copper's thermal conductivity and the RRR it is possible to estimate that their OFHC Cu had an RRR of 173, a believable value, Valois et al.[39] stating that some OFHC Cu can have RRR's as large as 500. Knowing that the stack length was 5.48 cm this allows calculation of the ITC for the 32 interfaces, plotted in Figure 8a. At 2 K the calculated Kaptiza lengths of the Pb come to 0.53 cm in the superconducting case and 0.376 cm in the normal state, both much larger than the 0.0050 cm average thickness of the Pb layers, and it is concluded that interfacial conductance dominates for the Pb. However, the Cu is different, here the calculated Kapitza length at 2 K is 0.319 cm and so almost equal to the 0.3175 cm Cu disk thicknesses. When

considering the Cu, both ITC and the bulk thermal conductivity must be included. The bulk Cu thermal resistivity will be in series with the thermal boundary resistance.

Not shown in Figure 8a is a first analysis that ignores the bulk Cu contribution and would have the phonons fitting to $T^3/90$ and the a-BRT to $32R_cA=1.48\ \Omega\text{-}\mu m^2$. As in the case of Challis and Cheeke's multi-layer stack a correction using the normal state is possible by subtracting out the normal state ITC and fitting the phonon contribution to the lowest temperature superconducting data point which gives that to go as $T^3/80$. The electronic contribution is then determined by fitting the sum of the phonon and a-BRT to the highest data point (subtracting the bulk Cu contribution) at 2.0 K giving $32R_cA=0.968\ \Omega\text{-}\mu m^2$ (for a single interface the average RcA is then $0.03025\ \Omega\text{-}\mu m^2$, the smallest value encountered so far, perhaps due to the vacuum casting used to create the stack) the results of which are those plotted in Figure 8a. Adding back in the series resistance of the normal state to the paralleled phonon plus electronic sum and plotting this again with the thermal boundary resistance as the y-axis results in Figure 8b, where it is seen that the combined sums (purple curve) extrapolate out to match the extrapolated normal state at T_c, showing the possibility that the contribution of the copper disk's thermal resistance can be extracted and used to obtain more accurate values for the phonon and electron interfacial contributions.

Barnes and Dillinger also measured three samples of Sn-Cu (one undesignated specimen reported in 1963[22] and two others designated as Sn-Cu1 and Sn-Cu2 in 1966[31]) between 1.3K and 2.0 K, but at 35% to 53% of Sn's T_c this falls in the regime where electron and phonon contributions to the ITC must both be considered. Simply fitting a power law to their data yields that in the superconducting state the ITC goes as $T^{2.87}$, $T^{2.59}$, and $T^{4.257}$ for the 1963 sample, sample Sn-Cu1, and sample Sn-Cu2, respectfully. Considering AMM predictions and the measured thermal resistance when in the normal-state along with the superconducting state, the authors concluded that for Sn-Cu interfaces the transfer of heat was dominated by electrons in both superconducting and normal states.

In the narrow temperature range of Barnes and Dillinger's data many overlapping combinations can be made to fit. For example, if for sample Sn-Cu1 a DMM coefficient of 4.14 K^4cm^2/W is assumed then a BRT contact resistance of 0.792 $\Omega\text{-}\mu m^2$ results in an apparently nice fit to the data, but so does a fit with 1.8 K^4cm^2/W coefficient and no electronic component, or conversely a BRT contact resistance of 0.473 $\Omega\text{-}\mu m^2$ and no phonon component. Similarly for Sn-Cu2 fits ranging from a purely phonon mechanism using $T^3/1.1$ to a purely electronic using 0.264 $\Omega\text{-}\mu m^2$ and values combined in between produce nice fits to the data. The authors took data in the normal state, with six data points with some scatter for Sn-Cu1 which does fit well enough to the expected the T^1 dependance and even extrapolates to coincide at T_c with the purely electronic prediction; imposing the normal-state slope sets the specific resistances for either the a-BRT or the NIS are presented in Figure 9. At low temperatures the NIS contribution is considerably smaller than the a-BRT, for example at 1 K ($0.27T_c$) the ITC for the NIS is just 19% that of the a-BRT. This requires the predicted phonon resistance to be much smaller if summed in parallel with the NIS contribution. A scaled Andreev analysis was not undertaken; it would require combination with either the NIS or BRT mechanisms to predict performance above and below T_c, and as was just seen, there is not sufficient fidelity to glean more information with any useful confidence. Regarding the other two Sn-Cu sample data of Barnes and Dillinger, the four points of the normal state data for Sn-Cu2 fit not even close

to an approximate T^1 power law, but instead to an unexpected $T^{3.47}$ and the extrapolations simply cannot be made to coincide at all. Analysis of the undesignated 1963 sample is similar but not identical to Sn-Cu1.

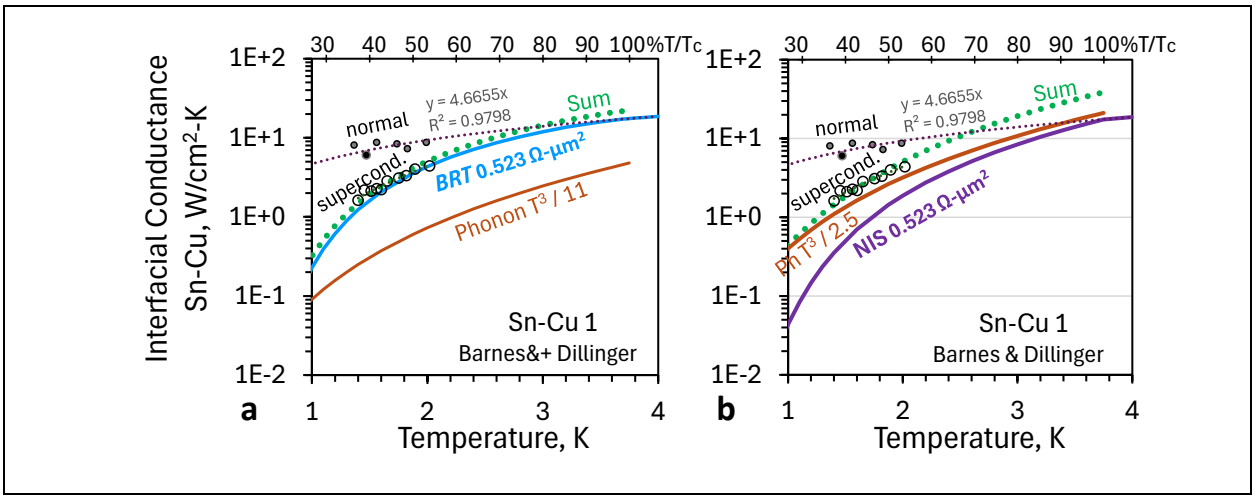


Figure 9 - Interfacial Thermal Conductance data converted form Barnes and Dillinger[31] interfacial thermal conductance measurements on sample Sn-Cu1, with fittings to the normal-state slope, and with the conductances added in parallel, considering: (a) adapted-BRT , (b) NIS.

Discussion

Inclusion of a phonon component at temperatures below $0.5T_c$ has been seen to be important and dominant below $0.2T_c$. The historical experimental thermal data included here appears to all be for "dirty" interfaces with impurities, defects, or an insulating layer. Present phonon transport theory does not well represent the nature across such dirty and thin interfaces. In the above analysis a T^3 dependence of the thermal conductance across an interface for heat carried by phonons has been assumed. A more complete consideration of the thermal conductivity in the bulk would also include the T^2 scattering of the phonons by electrons[40]. Future analysis should include such a term for interfacial transport, this will be needed at higher temperatures in the superconducting state, to predict when phonon transport becomes negligible. For electrons as heat carriers the analysis of the experimental data presented in Figure 1 through Figure 9 considered limiting the transport of heat by electrons using the Wiedemann-Franz law for interfaces by tunnelling or for the adapted BRT a limitation of electronic heat transport by impurity scattering. When considering bulk thermal conductivity the electrons can also be scattered by phonons which goes as T^{-2} and occurs over all temperatures[40]. A future analysis should also consider whether such a scattering mechanism is also important at superconductor to normal-metal interfaces.

With regard to tunneling transport, an Andreev mechanism requires a clean NS contact, and in the analysis presented here it was found necessary to scale this down to 1% or less of the full interfacial area. Across an insulating layer NIS tunneling can occur, and when in parallel permits consideration both above and below T_c. It also predicts a peak in interfacial conductance just below T_c which has been observed

in electrical resistivity measurements but this peak in ITC has not been evident in the admittedly quite limited thermal measurement data. The NIS and BRT mechanisms decrease monotonically as the temperature decreases, and especially when combined, can well fit all of the data both above and below T_c.

The application of the Wiedemann-Franz law, originally relating bulk electrical conductivity and bulk thermal conductivity, has been well established to apply to interfacial transport[9]. Electrical measurements determine the R_cA specific contact resistance or thermal measurements determine the slop $\mathbb{h}'(=L_o/R_cA)$ of the heat transfer coefficient with respect to temperature For clean interfaces involving sub-micron thick films this has been successfully predicted using the Electron Diffuse Mismatch Model (EDMM)[21]. Studies involving material pairs that constitute potentially superconducting elements include Nb-Cu[11], Al-Cu[41], Ir-Pd[10,42], V-Cu[43], Nb-Cu[43], and W-Cu[43]. Of this list [11] and [41] did thermal measurements while the rest did electrical measurements. All measured down to cryogenic temperatures but only Park et al.[43] took their samples down to a temperature (4.2 K) cold enough that would have rendered bulk V and Nb into the superconducting state; the authors state that due to the extreme thinness of their films (≤20 nm) and sandwiching them between the normal-metal Cu and ferromagnetic permalloy films of their test structures this entirely suppressed superconductivity at 4.2 K. Also all of the six material pairs listed had their interfacial contacts formed under vacuum and as such are clean NS boundaries, with the determined R_cA values ranging from 0.00051 to 0.00271 Ω-μm^2. The bulk "dirty" interfaces examined in Figure 2 through Figure 9 are one to two orders of magnitude larger in contact resistance than the measured clean thin film interfaces that align with EDMM values. It is concluded that EDDM theory only applies to clean boundaries.

All of the ITC equations given here have only depended upon the properties of the superconducting material. Presumably the normal-metal side has such a large number of free electrons that its particular properties do not matter. In a broad sense the gap formed in the superconductor is functioning as the energy filter that decreases the ITC as the temperature is decreased. Typical normal-metals have one to a few free electrons per atom, and is the case for all of the data examined here, however, it has been shown that doped semiconductors, with their lower densities of available electrons, can still function as the normal-metal in an NS contact[44]. While of less interest from a practical sense as a heat sink in a cryogenic thermal management system due to its inherently low thermal conductivity, it could be informative in shaping a theory that includes the normal side material's properties to examine Bismuth in a NS contact. Bi has a T_c below 0.53 mK[45] and as a semi-metal has a low ~3×10^{17} cm^{-3} carrier density[46] (only 1 electron per 100,000 atoms) and thus very few free electrons to interact with the superconducting side.

All of the experimental data considered have been for near-isothermal conditions where an average temperature can be used for comparison with the various theories. Barnes and Dillinger[22] limited in their experiments the maximum ΔT to 0.1 K which in the worst case corresponds to a small $\Delta T/T$ of 0.075 and explicitly looked for a difference in the interfacial thermal resistance when flipping the heat flow direction, finding none. However, for large temperature jumps using an average temperature cannot be readily assumed and rectification effects[47] will become important.

At $T > T_c/2$ it is difficult to determine how much of the interfacial thermal conductance is due to Andreev, adapted BRT, or NIS mechanisms just from heat transfer data alone. At lower temperatures for $T < T_c/5$, Andreev, the adapted BRT, and the modified Bessel function of the second kind used in the NIS expression will all decay as $e^{(-\Delta/k_B T)}$. Their pre-factors vary differently, with the thermal conductance for Andreev and NIS going as $1/\sqrt{T}$, and the adapted BRT as$1/T$. These are not too different and unfortunately the phonon component is likely to dominate at low temperatures. If the normal-state slope of the ITC is known then, as illustrated in Figure 9, then the differing values calculated at low temperatures might allow experimentally distinguishing BRT from NIS dependence experimentally if the phonon and Andreev components can be minimized. From the experimental data, just pairing the NIS mechanism with phonon transport does not well fit to that data, the NIS contribution decreases too quickly as the temperature is lowered. This would indicate that any NIS transport is likely acting in concert with Andreev or BRT mechanisms.

Distinguishing the true thermal transport mechanisms for superconductor to normal-metal contacts will require simultaneous measurements of both electrical and thermal interfacial resistances, covering temperatures from above T_c down below $0.2T_c$, for interfaces fabricated in room air with and without an appropriate solder flux, and compared to clean interfaces fabricated under vacuum.

Conclusion

Experimental interfacial thermal conductance data from the literature for superconductor to dissimilar normal-metal interfaces was fitted to the theoretical expressions of Andreev, Griffin-Maki, and, with the application of the Wiedemann-Franz law for boundaries between dissimilar materials adaptation of Bardeen, Rickayzen, and Teword's equation and, as given by Giaever and Megerle for NIS contacts. Use of Wiedemann-Franz reduces the required fitting constant to just a single specific contact resistance. It was found that the asymptotic equations of Griffin and Maki did not fit as well compared to the other theories. The fact that the Andreev thermal interfacial conductance required scaling to about 1% or less of the contact area suggests that 99% or more of the contact has a different transport mechanism. When paired with a parallel NIS tunneling, good fits to the data were found, along with a peak in the ITC just below T_c that was not evident in the (admittedly sparse) thermal data but does appear in some electrical conductance (non-thermal) measurements. The adapted BRT equation fittings to the thermal data produced R_cA values ranging from 0.018 to 0.72 Ω-μm^2. Comparing this to the 0.001-0.002 Ω-μm^2 typical values measured in electrical (non-thermal) tests on NN samples whose interfaces were formed on pre-sputtered vacuum deposited samples indicates that the thermal data, taken on samples largely prepared in ambient air, can be presumed to be "dirty." When summed with a T^3 phonon transport mechanism this explains why historically researchers found their data fitting to more than T^3 to T^6behavior over the limited range of their thermal data. The contribution to the ITC due to electrons dominating above 50% of T_c. For 0.2 < T/T_c< 0.5 both transport mechanisms must be accounted for to align with experiment. The simplest approach for those seeking to produce thermal predictions based on a narrow range of data would be to use the adapted BRT (Equation 6) in parallel to the phonons, since only two constants are needed to cover the entire range from above T_c down into the superconducting regime, namely the

phonon interfacial thermal boundary resistance constant B (as used in $1/G_b = R_b = B/T^3$), and the specific contact resistance R_cA or alternatively derived from the equivalent heat transfer constant $\mathbb{h}' = L_o/R_cA$ with $\mathbb{h}'$ directly read as the slope constant of the ITC versus temperature plot when both materials are in the normal state.

Appendix: Useful Approximations To The Adapted BRT Equation

To better than 2% for $y > 4.6$ ($T < 0.38\ T_c$ for a superconductor that follows $\Delta = 1.76 k_B T_c$; but $T < 3.28\ K$ for Pb) Equation 6 approximates to:

$$\left(R_{th,es}^{BCS}\ A\right)^{-1} = {G_{th,es}^{BCS}}\Big/{A} \approx\ 4\left({k_B^2}/{e^2}\right)\left(\frac{T}{R_c^{BRT} A_c^{BRT}}\right) exp(-y)\{1 + y + \tfrac{1}{2}y^2\}$$

Equation 9.

For $\Delta \gg k_B T$ this further approximates to

$\left(R_{th,es}^{BCS}\ A_c^{BRT}\right)^{-1} = {G_{th,es}^{BCS}}\Big/{A_c^{BRT}} \approx\ 2(k_B^2)\left(\frac{T}{e^2 R_c^{BRT} A_c^{BRT}}\right)\left(\frac{\Delta}{k_B T}\right)^2 exp\left(\frac{-\Delta}{k_B T}\right)$ with Δ in Joules, T in Kelvin, and k_B in Joules per Kelvin.

In terms of thermal resistance $R_{th,es}^{BCS}$ [K/W] $\approx \frac{1}{2\left(k_B^2\right)}\left(\frac{e^2 R_c^{BRT}}{T}\right)\left(\frac{k_B T}{\Delta}\right)^2 exp\left(\frac{\Delta}{k_B T}\right)$

Acknowledgements

The author would like to thank Drs. K. Myers, A. Erol, J. Shipman, and L. Freidman, and Mr. A. Mamoozadeh for their comments during the analysis presented here. The encouragements of Drs. G. Boyd, A. Pesetski, and M. Sherwin are gratefully acknowledged.

Funding

None.

REFERENCES

[1] G. E. Blonder, M. Tinkham, and T. M. Klapwijk, Transition from metallic to tunneling regimes in superconducting microconstrictions: Excess current, charge imbalance, and supercurrent conversion, Phys. Rev. B 25, 4515 (1982); DOI: https://doi.org/10.1103/PhysRevB.25.4515

[2] A. F. Andreev, The Thermal Conductivity of the Intermediate State in Superconductors, Soviet Physics-JETP, 19(5) 1228-1232 (1964)

[3] P. Bonnard, P. Laeng, J-M Suter & L. Rinderer, Thermal resistance of a normal/superconductor interphase boundary in high-purity lead. J Low Temp Phys 47, 255–269 (1982). https://doi.org/10.1007/BF00683730 (Note that the published paper has a typographical error, in that the Fermi wavevector should be squared. The calculated curve comparison to their Pb data appears to correctly use the k_F^2 in the analysis presented in their Fig. 6.)

[4] P. Bonnard, L. Rinderer, Thermal resistance of normal - superconductor interphase boundaries, Physica B: Condensed Matter Volumes 194–196, Part 2, 2 February 1994, Pages 1509-1510 https://doi.org/10.1016/0921-

4526(94)91254 (Note that the published paper also has a typographical error, in that the pre-factor of 4 should be 2. The calculated curve comparison to their Sn data appears to correctly use the value of 2 in the analysis presented in their Fig. 2.)

[5] A. Griffin, K. Maki, Heat flow between normal and superconducting regions, Physics Letters, 23(7) 429-430 (1966); https://doi.org/10.1016/0031-9163(66)91077-8

[6] J. Bardeen, G. Rickayzen, and L. Tewordt, Theory of the Thermal Conductivity of Superconductors, Phys. Rev. 113, 982 (1959). https://doi.org/10.1103/PhysRev.113.982

[7] L. J. Challis and J. D. N. Cheeke, Thermal conduction across copper-lead-copper sandwiches at helium temperatures 1964 Proc. Phys. Soc. 83 109; DOI 10.1088/0370-1328/83/1/314

[8] B. Schumann, F. Nitsche, and G. Paasch, Thermal Conductance of Metal Interfaces at Low Temperatures, Journal of Low Temperature Physics, 38(1/2) 167-189 (1980). https://doi.org/10.1007/BF00115274

[9] G. D. Mahan, M. Bartkowiak, Wiedemann–Franz law at boundaries, Appl. Phys. Lett. 74, 953–954 (1999); https://doi.org/10.1063/1.123420

[10] R. B. Wilson and David G. Cahill, Experimental Validation of the Interfacial Form of the Wiedemann-Franz Law, Phys. Rev. Lett. 108, 255901 (2012); DOI: https://doi.org/10.1103/PhysRevLett.108.255901

[11] Ramez Cheaito, Khalid Hattar, John T. Gaskins, Ajay K. Yadav, John C. Duda, Thomas E. Beechem, Jon F. Ihlefeld, Edward S. Piekos, Jon K. Baldwin, Amit Misra, Patrick E. Hopkins, Thermal flux limited electron Kapitza conductance in copper-niobium multilayers, Appl. Phys. Lett. 106, 093114 (2015); https://doi.org/10.1063/1.4913420

[12] T.V. Blank, Y.A.Gol'dberg, Mechanisms of current flow in metal-semiconductor ohmic contacts. Semiconductors 41, 1263Hardin–1292 (2007); https://doi.org/10.1134/S1063782607110012

[13] J. P. Gambino and E. G. Colgan, Silicides and ohmic contacts, Materials Chemistry and Physics 52(2), 99-146 (1998); https://doi.org/10.1016/S0254-0584(98)80014-X

[14] A. Kikuchi, Calculation of Ohmic Contact Resistance at a Metal/Silicon Interface, physica status solidi (a) 175(2) 623-629 (1999); https://doi.org/10.1002/(SICI)1521-396X(199910)175:2<623::AID-PSSA623>3.0.CO;2-R

[15] Ashish Baraskar, A. C. Gossard, and Mark J. W. Rodwell, Lower limits to metal-semiconductor contact resistance: Theoretical models and experimental data, Journal of Applied Physics 114, 154516 (2013); http://dx.doi.org/10.1063/1.4826205

[16] G. L. Harding, A. B. Pippard, and J. R. Tomlinson, Resistance of Superconducting-Normal Interfaces, Proceedings of the Royal Society of London. Series A, Mathematical and Physical Sciences Vol. 340 (1620) 1-31 (1974) https://www.jstor.org/stable/i204440

[17] Ivar Giaever and Karl Megerle, Study of Superconductors by Electron Tunneling, Phys. Rev. 122(4) 1101-1111 (1961); DOI: https://doi.org/10.1103/PhysRev.122.1101

[18] S. Strässler r and P. Wyder, Thermal Conductivity and Electron Scattering at Interphase Boundaries in a Superconductor, Phys. Rev. Letters 10, 225 (1963); DOI: https://doi.org/10.1103/PhysRevLett.10.225

[19] E. T. Swartz and R. O. Pohl, Thermal resistance at interfaces, Appl. Phys. Lett. 51, 2200 (1987); doi: 10.1063/1.98939

[20] E. T. Swartz and R. O. Pohl, Thermal boundary resistance, Rev. Mod. Phys. 61(3), 605 (1989); DOI: https://doi.org/10.1103/RevModPhys.61.605

[21] Jie Chen, Xiangfan Xu, Jun Zhou, and Baowen Li, Interfacial thermal resistance: Past, present, and future, Rev. Mod. Phys. 94, 025002 (2022); DOI: https://doi.org/10.1103/RevModPhys.94.025002

[22] L. J. Barnes and J. R. Dillinger, Thermal Boundary Resistance Between Some Superconducting and Normal Metals, Physical Review Letters, 10(7) 287-289 (1963); DOI: https://doi.org/10.1103/PhysRevLett.10.287

[23] R. F. Gasparovic, B. N. Taylor, R. E. Eck, Temperature dependence of the superconducting energy gap of Pb, Solid State Communications 4, 59 (1966) https://doi.org/10.1016/0038-1098(66)90106-2

[24] T.P. Sheahen, Rules for the Energy Gap and Critical Field of Superconductors, Physical Review 149(1) 368-370 (1966); DOI: https://doi.org/10.1103/PhysRev.149.368

[25] J. Bardeen, L. N. Cooper, and J. R. Schrieffer, Theory of Superconductivity, Phys. Rev. 108(5) 1175-1204 (1957) ; DOI: https://doi.org/10.1103/PhysRev.108.1175

[26] P. Townsend and J. Sutton, Investigation by Electron Tunneling of the Superconducting Energy Gaps in Nb, Ta, Sn, and Pb, Phys. Rev. 128, 591 (1962) DOI: https://doi.org/10.1103/PhysRev.128.591

[27] D.J. Van Harlingen, Thermoelectric generation of charge imbalance at a superconductor-normal metal interface. J Low Temp Phys 44, 163–176 (1981). https://doi.org/10.1007/BF00115081

[28] Thomas Y. Hsiang and John Clarke, Boundary resistance of the superconducting-normal interface

Phys. Rev. B 21(3), 945-955 (1980); DOI: https://doi.org/10.1103/PhysRevB.21.945
[29] L. J. Challis and J. D. N. Cheeke, The thermal conductance of copper-lead-copper sandwiches at liquid helium temperatures, Physics Letters 5(5) 305-307 (1963); https://doi.org/10.1016/S0375-9601(63)93965-3
[30] J. Clarke, S.M. Freake, M.L. Rappaport and T.L. Thorp, A new experimental technique for determining the BCS interaction parameter in normal metals, Solid State Communications 11(5), 689-693 (1972); https://doi.org/10.1016/0038-1098(72)90488-7
[31] L. J. Barnes and J. R. Dillinger, Thermal Resistivity at Pb-Cu and Sn-Cu Interfaces between 1.3 and 2.1°K, Physical Review 141(2) 615-620 (1966); DOI: https://doi.org/10.1103/PhysRev.141.615
[32] M. Hansen and K. Anderko, Constitution of Binary Alloys, 2nd Ed. (Genium Publ. Comp., Schenectady, NY: 1985).
[33] Christian Brand, Tobias Witte, Mohammad Tajik, Jonas D. Fortmann, Birk Finke, Herbert Pfnür, Christoph Tegenkamp, Michael Horn-von Hoegen, Thermal boundary conductance under large temperature discontinuities of ultrathin Pb(111) films on Si(111), Appl. Phys. Lett. 127, 172202 (2025); https://doi.org/10.1063/5.0291617
[34] H. Montgomery, The thermal conductivity of lead at low temperatures, Proceedings of the Royal Society A , 244, 85-100 (1958); https://doi.org/10.1098/rspa.1958.0027 [See also curve 24 for Pb in: Y.S. Touloukian, Vol. 01 Thermophysical Properties of Matter, (IFI/Plenum, New York-Washington: 1970); https://apps.dtic.mil/sti/citations/ADA951935]
[35] W. Odoni, P. Fuchs, and H. R. Ott, Size effect on the lattice thermal conductivity of lead single crystals Phys. Rev. B 28, 1314 (1983); DOI: https://doi.org/10.1103/PhysRevB.28.1314
[36] A. Wawro, The electron mean free path and superconductivity in Cu/Pb modulated films, Journal of Physics: Condensed Matter, 5(44) 8391-8402 (1993); DOI 10.1088/0953-8984/5/44/025
[37] Robert O. Pohl, Xiao Liu, and EunJoo Thompson, Low-temperature thermal conductivity and acoustic attenuation in amorphous solids, Reviews in Modern Physics 74 991 -1013 (2002) DOI: https://doi.org/10.1103/RevModPhys.74.991.
[38] J. G. Hust, A. B. Lankford, Thermal conductivity of aluminum, copper, iron, and tungsten for temperatures from 1 K to the melting point, NBSIR-84/3007, National Bureau of Standards, Boulder, CO (USA) 1984; https://www.govinfo.gov/content/pkg/GOVPUB-C13-5dca61206b094d8b3a54099ebcff1baa/pdf/GOVPUB-C13-5dca61206b094d8b3a54099ebcff1baa.pdf
[39] J. J. Valois, G. F. Nellis, J. M. Pfotenhauer, Characterization of the thermal properties of OFHC copper at cryogenic temperature, IOP Conf. Series: Materials Science and Engineering 130,1 012167 (2024); doi:10.1088/1757-899X/1301/1/012167
[40] F Koechlin and B Bonin, Parametrization of the niobium thermal conductivity in the superconducting state, Supercond. Sci. Technol. 9 (6) 453–460 1996; DOI 10.1088/0953-2048/9/6/003
[41] Byan C. Gundrum, David G. Cahill, and Robert S. Averback, Thermal conductance of metal-metal interfaces, Phys. Rev. B 72, 245426 (2005); DOI: https://doi.org/10.1103/PhysRevB.72.245426
[42] R. Acharyya, H. Y. T. Nguyen, R. Loloee, J. W. P. Pratt, J. Bass, S. Wang, and K. Xia, Specific resistance of Pd/Ir interfaces, Appl. Phys. Lett. 94, 022112 (2009); https://doi.org/10.1063/1.3072365.
[43] W. Park, D. V. Baxter, S. Steenwyk, I. Moraru, W. P. Pratt, Jr., and J. Bass, Measurement of resistance and spin-memory loss (spin relaxation) at interfaces using sputtered current perpendicular-to-plane exchange-biased spin valves, Phys. Rev. B 62, 1178 (2000); DOI: https://doi.org/10.1103/PhysRevB.62.1178
[44] Emma Mykkänen, Janne S. Lehtinen, Leif Grönberg, Andrey Shchepetov, Andrey V. Timofeev, David Gunnarsson, Antti Kemppinen, Antti J. Manninen, Mika Prunnila, Thermionic junction devices utilizing phonon blocking, Science Advances 6 (15) (2020); https://doi.org/10.1126/sciadv.aax9191
[45] O. Prakash, A. Kumar, A. Thamizhavel, S. Ramakrishnan, Evidence for bulk superconductivity in pure bismuth single crystals at ambient pressure, Science 355(6320) 52-55 (2016); DOI: 10.1126/science.aaf8227
[46] M. V. Likholetova, E. V. Charnaya, E. V. Shevchenko, and Yu. A. Kumzerov, Superconductivity of the Bi–Sn Eutectic Alloy. Physics of the Solid State, 63(2), 232–236 (2021); https://doi.org/10.1134/S1063783421020153
[47] F. Giazotto and F. S. Bergeret, Thermal rectification of electrons in hybrid normal metal-superconductor nanojunctions, Appl. Phys. Lett. 103, 242602 (2013); https://doi.org/10.1063/1.4846375